Multiple Steady States in an Isothermal, Integral Reactor: The Catalytic Oxidation of Carbon Monoxide Over Platinum-Alumina

Stable isothermal multiplicities were observed during carbon monoxide oxidation in an integral reactor, filled with alumina supported platinum catalysts. The multiplicities were investigated in the conversion-temperature, conversion-inlet carbon monoxide concentration and conversion-mass flow rate domains.

The region of multiplicities was found to widen significantly upon catalyst aging which enhanced the pellets' diffusive resistances.

Several intermediate stable steady states were found between the highest and lowest steady states, both experimentally and theoretically.

All the above phenomena could be well interpreted by the interactions of the kinetics of carbon monoxide oxidation with intrapellet diffusion resistances.

L. LOUIS HEGEDUS
SE H. OH
and
KENNETH BARON

General Motors Research Laboratories
Warren, Michigan 48090

SCOPE

The oxidation of carbon monoxide over noble metal catalysts is an important part of the catalytic control of automobile emissions. A voluminous and fast growing literature deals with this application, which was recently reviewed by Wei (1975*a*, *b*) and previously by several of the references therein.

Besides its technical importance, the catalytic oxidation of carbon monoxide over platinum seems to provide continuing fascination and puzzlement to experimentalists and theoreticians alike. Despite the large number of papers dealing with the subject, the kinetics of the reaction is still unsettled. However, one major feature seems to be the change from positive order in carbon monoxide at low carbon monoxide concentrations to negative order at high carbon monoxide concentrations (for example, Voltz et al., 1973; McCarthy et al., 1975).

Negative order reactions, when coupled with intrapellet diffusion resistances, have been predicted to give rise to peculiar phenomena, such as isothermal effectiveness factors above unity and multiple solutions (Roberts and Satterfield, 1966; Schneider and Mitschka, 1966; for a recent review, see Aris, 1975). Indeed, when the bimolecular Langmuir-Hinshelwood type of rate expression of Voltz et al. (1973) was employed in the calculations, Wei and Becker (1975) and Smith et al. (1975) predicted multiple solutions for carbon monoxide oxidation in porous catalyst pellets as a result of diffusion-reaction interactions. According to those calculations, however, the carbon monoxide concentration has to be larger than about 10 vol % to predict multiplicity.

Experimental work on multiplicities in chemically reacting systems has been reviewed recently by Schmitz (1975). For carbon monoxide oxidation in a single, isothermal, porous platinum-alumina catalyst pellet, multiple steady states were first observed by Wicke and collaborators (for example, Beusch et al., 1972). They suggested that the multiplicities were caused by the interactions between kinetics and chemisorption rates, and not by any diffusion-reaction mechanism.

Apparently, surface phenomena indeed play a role in the unusual behavior of the carbon monoxide-platinum system (for example, Cardoso and Luss, 1969; Hugo, 1970; Hugo and Jakubith, 1972; Dauchot and Van Cakenberghe, 1973; McCarthy et al., 1975; Dagonnier and Nuyts, 1976). For porous catalysts with an appreciable internal diffusion resistance, such as the catalysts employed in this paper, we will show that the multiplicities may be interpreted by diffusion-reaction interferences.

A great deal of experimental and theoretical work has been devoted to the study of carbon monoxide oxidation over platinum (or palladium) in adiabatic, integral reactors (for example, Padberg and Wicke, 1967; Fieguth and Wicke, 1971; Eckert et al., 1973; Votruba and Hlavacek, 1974; Votruba, et al., 1976). In this paper, the authors report on isothermal, integral reactor studies of carbon monoxide oxidation over porous platinum-alumina catalysts. The experiments were carried out on catalysts and reactors with well-characterized properties such that a direct comparison of the experimental data with diffusion-reaction theory was possible. This, in turn, allowed some conclusions about the nature of diffusion-reaction interferences and about their effects on multiplicities in an isothermal reactor.

CONCLUSIONS AND SIGNIFICANCE

Fresh and aged platinum-alumina automotive catalysts were characterized by a number of physical and chemical techniques to provide input parameters for mathematical models used to analyze their behavior. The pellets were described by a multizone model which allows for different reactivities and diffusivities in four different zones along the pellet radii.

An isothermal, integral reactor was constructed and used to oxidize carbon monoxide under controlled conditions. The conversion was monitored as a function of temperature, inlet carbon monoxide concentration, or mass flow rate.

A mixing cell model was employed to describe the reactor's conversion behavior. The conservation equation which

describes the individual catalyst pellets was solved by the Ritz-Galerkin technique. A transient model was also developed to simulate the stable steady states which were discovered between the highest and lowest solutions.

Conversion-temperature and conversion-inlet concentration experiments showed a pronounced range of reactor multiplicities. Comparison of the data with the diffusion-reaction model indicated that the multiplicities are due to the interactions of the negative-order kinetics for carbon monoxide oxidation with the diffusive resistances of the catalyst pellets.

The range of multiplicities was found to widen upon partial aging of the catalysts. These changes were easily interpreted by the diffusion-reaction model.

More then two stable steady states were found in the isothermal, integral reactor, both experimentally and theoretically. By a properly chosen sequence of experimental conditions, it was possible to generate stable steady states in the inside of the conversion-temperature, conversion-inlet concentration and conversion-mass flow rate hysteresis envelopes. These intermediate stable steady states are the result of diffusion-reaction interactions and were easily predictable by the dynamic model.

Addition of water vapor to the feed stream eliminated the isothermal multiplicities, at least within the carbon monoxide concentration range of this work, apparently by reducing the carbon monoxide-platinum adsorption equilibrium constant in the rate equation.

EXPERIMENTAL PART

Four alumina supported platinum catalysts have been selected for the experiments (Table 1). The fresh catalysts A1 and B1 have only slightly different characteristics. Catalyst A2 was aged for 1 000 hr in the exhaust of a dynamometer mounted V-8 automobile engine, while catalyst B2 was aged for 57 hr on a similar engine but with a fuel which was enriched in phosphorus to accelerate the aging process. The two catalysts are distinguished by the fact that while the poisons do not seem to plug the pores of catalyst B2, catalyst A2 is surrounded by a partially impervious layer with a reduced diffusivity.

The noble metal dispersions for the fresh catalysts were determined by carbon monoxide chemisorption. The pore volumes (V_{macro}, V_{micro}), integral averaged pore radii ($\bar{r}_{macro}$, $\bar{r}_{micro}$), and solid densities (ρ_s) were determined by ultrahigh pressure mercury porosimetry.

Platinum impregnation depths can be conveniently measured by stannous chloride staining, while the poison penetration depths were determined from electron microprobe observations of cross sections of the catalyst pellets. Both the noble metal impregnation profiles and the poison profiles were reasonably sharp along the pellet radii, such that a simple picture of the catalyst pellets could be constructed (Hegedus and Summers, 1975; Hegedus and Cavendish, 1976), as shown in Figure 1. Zone 4 (if present) is partially obstructed and poisoned, zone 3 (if present) is poisoned, zones 2, 3 and 4 are impregnated by platinum, and zone 1 is left unimpregnated. The dimensions of these zones for the catalysts A1, A2, B1, and B2 are shown in Table 1.

The effective diffusivity of carbon monoxide in the unobstructed portions of the catalyst pellets was calculated from the random pore diffusivity model of Wakao and Smith (Smith, 1970) which appears to be well suited for the bimodally distributed pore sizes of the alumina supports used here. The pore size distributions required by this model were obtained by ultrahigh pressure mercury porosimetry. The diffusivity across the obstructed zone 4 was determined from diffusion limited reactivity measurements, by adjusting D_4 to the fraction of D_2 which properly fits those data (Hegedus and Cavendish, 1976).

The integral reactor used for the experiments is depicted Figure 2. It has ben described previously by Hege-

TABLE 1. CHARACTERISTICS OF THE CATALYSTS EMPLOYED AND PARAMETERS USED IN THE COMPUTATIONS

	A1	A2	B1	B2
State	Fresh	Aged*	Fresh	Aged*
Pt (wt %)	0.086	0.060 (est.)	0.089	0.060 (est.)
Pt dispersion (%)	72	10 (est.)	53	10 (est.)
a_2 (cm^2 Pt/cm^3 pellet)	5 530	588 (est.)	6 569	791 (est.)
a_3 (cm^2 Pt/cm^3 pellet)	0	0	0	40 (est.)
Poison content				
Pb (wt %)	0	1.31	0	0
P (wt %)	0	0.39	0	0.95
V_{macro} (cm^3/g)	0.120	0.070	0.054	0.060
V_{micro} (cm^3/g)	0.510	0.515	0.530	0.470
$\bar{r}_{macro}$ (Å)	11 406	13 099	8 207	7 377
$\bar{r}_{micro}$ (Å)	115	220	127	130
ρ_s (g/cm^3)	3.60	3.61	3.6	3.6
ρ_p (g/cm^3)	1.102	1.160	1.160	1.238
s (m^2/g)	90	57	86	64
R (cm) (arithmetic mean)	0.1777	0.1766	0.1829	0.1851
$R - r_3$ (cm)	0	0.0007	0	0
$R - r_2$ (cm)	0	0.0013	0	0.0106
$R - r_1$ (cm)	0.0215	0.0204	0.0143	0.0165
$D_1 = D_2 = D_3$ (cm^2/s)†	0.0482	0.0589	0.0346	0.0346
D_4 (cm^2/s)	0.0482	0.00393	0.0346	0.0346

* See text for a description of the aging process.
† Computed from the random pore model of Wakao and Smith (Smith, 1970), and given here at 1 atm and 838°K. D increases with the 1.40th power of T.

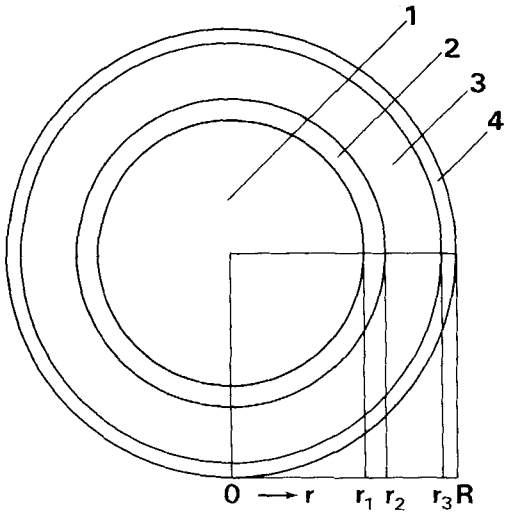

Zone 1: Unimpregnated Core

Zones 2, 3, 4: Noble Metal Impregnated Shell

Zone 3: Poisoned Shell

Zone 4: Partially Impervious Deposit

Fig. 1. Schematic diagram of the cross section of an aged catalyst pellet.

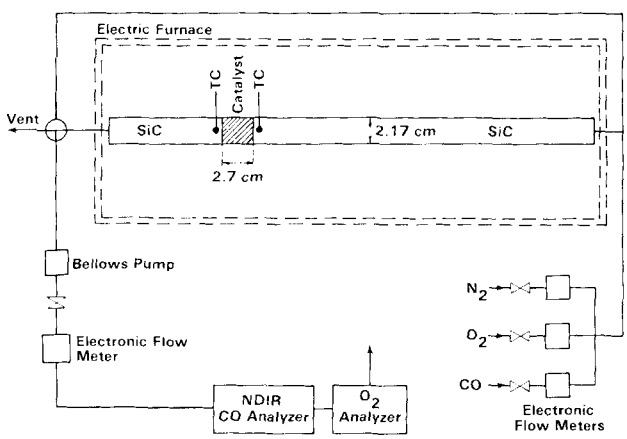

Fig. 2. Schematics of the reactor system.

dus and Cavendish (1976). The catalytically active section is sandwiched between two silicon carbide layers (silicon carbide particles serve here as an inert heat transfer medium and also to provide for a plug flow behavior). The stainless steel reactor tube is heated by an electric furnace, and thermocouples are used to monitor the temperature at the inlet and outlet plane of the reactive section. The reactive section has a total volume of 10.0 cm^3, carefully packed to well-measured void fractions.

About 2 vol % inlet oxygen concentration was used for all the experiments. Since the inlet carbon monoxide concentrations were kept low (in the 0.2 to 0.4 vol % range to ensure near isothermal operation), the large stoichiometric excess of oxygen eliminated the need for writing a separate conservation equation for oxygen.

While strict isothermicity could not be ensured (depending on the operating conditions, there was a slight temperature rise from the inlet to the outlet of the reactive section, in the order of about 5° to 15°C), a careful analysis of the results showed that the slight nonisothermal behavior did not significantly interfere with the conclusions of this paper. This is due to the fact that where kinetic control prevailed (low conversions), the heat generation was minimal, and where measurable heat generation occurred (high conversions), the data were usually safely in the region where transport limitations prevailed. As discussed later, the calculations included an account for any differences between inlet and outlet reactor temperatures.

In an attempt to ensure that the chemical state of the catalysts is reproducible at the beginning of each experiment, the catalytic reactor was first heated in a flowing mixture of 2 vol % oxygen and 0.3 vol % carbon monoxide until the temperature reached about 500°C. After 30 min at this temperature, the reactor was cooled in the above gas stream to room temperature. The appropriate reaction feed stream was then selected, and the reactor was stabilized at the temperature of the particular experiment. Owing to the sensitivity of the intrinsic rate constant k_o to minor irreproducibilities in the pretreatment procedure, ak_o was modified slightly from run to run to agree with the low conversion (that is, kinetically limited) end of the data.

THEORETICAL PART

The concentration of carbon monoxide in the catalyst pellet depicted by Figure 1 is described by the following equations (see, for example, Hegedus and Cavendish, 1976, for more detail):

$$\frac{1}{r^2}\frac{d}{dr}\left\{ D(r)r^2\frac{dc}{dr} \right\} - a(r)\tilde{R} = 0 \qquad (1)$$

The boundary conditions are

$$\frac{dc}{dr}(r_1) = 0 \qquad (2)$$

$$\frac{dc}{dr}(R) = \frac{k_m}{D(R)}[c_\infty - c(R)] \qquad (3)$$

At the interfaces r_2 and r_3, both the fluxes and concentrations are continuous:

$$D(r_{2-})\frac{dc}{dr}(r_{2-}) = D(r_{2+})\frac{dc}{dr}(r_{2+}) \qquad (4)$$

$$D(r_{3-})\frac{dc}{dr}(r_{3-}) = D(r_{3+})\frac{dc}{dr}(r_{3+}) \qquad (5)$$

$$c(r_{2-}) = c(r_{2+}) \qquad (6)$$

$$c(r_{3-}) = c(r_{3+}) \qquad (7)$$

For our problem, D and a are piecewise constant and are defined as follows:

$$D_1 = D_2 = D_3 \geqq D_4 \qquad (8)$$

$$a_1 = a_4 = 0 \qquad (9)$$

$$a_2 = \text{finite},\ a_3 = 0 \text{ or finite } (a_2 >> a_3) \qquad (10)$$

where D_1 is the effective diffusivity in zone 1, a_1 is the local noble metal surface area in zone 1, etc.

As discussed in the introduction, the kinetics of carbon monoxide oxidation over platinum catalysts is subject to considerable variation of opinion among the numerous papers available in the literature. Instead of reviewing the field here, we quote experiments with a recycle reactor in our laboratories which indicated that, at least in the concentration range of our experiments, an approximate correlation of the rate data is possible if one uses the bimolecular Langmuir-Hinshelwood expression to which the rate equation of Voltz et al. (1973) collapses

TABLE 2. PARAMETERS CORRESPONDING TO THE VARIOUS EXPERIMENTS

Fig. →	3	4	5	6	7	8†	10, 11	12, 13, 14	15	16
Catalyst	A1	A2	B1	B2	A1	A2	A2	A2	A2	A2
$a\,k_o \times 10^{-15}$	4.4	2.3	5.9	6.3*	5.0	1.5	1.8	1.8	2.3	—
T_{in} (°C)	Varies	Varies	Varies	Varies	201	215	Varies	215	216	Varies
ϵ	0.45	0.46	0.39	0.40	0.35	0.42	0.40	0.42	0.43	~0.4
$c_{O_2,in}$ (vol %)	1.99	1.97	1.97	1.97	1.96	1.96	2.02	1.96	1.96	~1.5
$c_{CO,in}$ (vol %)	0.302	0.290	0.307	0.318	Varies	Varies	0.291	Varies	0.307	~0.3
Q_p (g/s)	0.110	0.109	0.112	0.110	0.111	0.111	0.108	0.111	Varies	~0.3

* Value given for a_3k_o. For this catalyst, $a_3k_o = 0.32 \times 10^{15}$.
† Curve b in Figure 8 employs $D_4 = D_2/10$, $ak_o = 1.8 \times 10^{15}$.

if only carbon monoxide and oxygen are present in the feed stream. However, we found that the energy of activation and the carbon monoxide adsorption equilibrium constant needed some modifications with respect to the values given by Voltz et al. (1973) to agree with our experiments where only carbon monoxide and oxygen were present in the feed stream.

The rate equation we use in the following calculations, then, becomes

$$\tilde{R} = \frac{k_o T \exp(-E/R_g T)\, c\, c_{O_2}}{[1 + K_o T \exp(H/R_g T) c]^2} \left(\frac{\text{mole}}{\text{cm}^2\,\text{Pt s}}\right) \quad (11)$$

where

$$k_o \approx 10^{12} \quad (12)$$

(ak_o was adjusted slightly to fit the low T, kinetic part of the particular experiments, as shown in Table 2), and

$$E = 15\,000 \text{ cal/mole} \quad (13)$$

$$K_o = 4.5 \times 10^5 \text{ cm}^3/(\text{mole °K}) \quad (14)$$

$$H = 2\,000 \text{ cal/mole} \quad (15)$$

It is worth mentioning that reported values of E vary widely among different investigators. While very low values indicate strong diffusional resistances, high values can also result from diffusion interferences with Langmuir-Hinshelwood kinetics. For example, for the particular porous platinum-alumina catalysts at hand, the effective value of E goes through a maximum as T increases. This makes it particularly difficult to use the effective energy of activation as a diagnostic tool for diffusion interferences if negative reaction orders can occur.

Equations (1) to (7) were solved for the individual catalyst pellets by the Ritz-Galerkin technique (a recent description of the application of this technique to composite catalyst pellets is given by Hegedus and Cavendish, 1976, and a general description by Finlayson, 1972). It has the advantage that the trial function is automatically satisfied at the zone boundaries, and thus all the zones of the pellet can be modeled by a single differential equation. The convenience of using it is especially apparent when more than one of the zones is catalytically active.

The integral reactor was simulated by a cascade of mixing cells. Owing to the isothermal nature of the system, only axial mixing cells were used. Since the catalyst bed is about 8 pellet diameters long, eight mixing cells were chosen. However, trial solutions with six and ten mixing cells showed no significant differences.

It is worth reproducing here the conservation equation around mixing cell j:

$$Q[c_x(j-1) - c_x(j)] + 3k_m V_{cell} \frac{1-\epsilon}{R} [c(R,j) - c_x(j)] = 0 \quad (16)$$

$c_x(j)$ is unknown at this time. It is determined by the solution of Equations (1) to (7) which, in turn, require the knowledge of $c_x(j)$ in Equation (3). The necessity of an iterative procedure can be circumvented by expressing $c_x(j)$ from Equation (16):

$$c_x(j) = \frac{c_x(j-1) + \alpha c(R,j)}{1+\alpha} \quad (17)$$

where

$$\alpha = \frac{3V_{cell}(1-\epsilon)k_m}{QR} \quad (18)$$

Equation (17) can now be substituted into (3) to yield

$$\frac{dc}{dr}(R) = \frac{k_m}{D_4(1+\alpha)} [c_x(j-1) - c(R,j)] \quad (19)$$

which now allows the solution of the single-pellet problem without iteration. This approach has been recently discussed by Finlayson (1974).

Owing to the slight axial temperature variation in the actual reactor experiments, the measured axial temperature rise was proportioned among the mixing cells in the calculations.

The external mass transfer coefficient of carbon monoxide, k_m, was calculated from the de Acetis-Thodos correlations (as given by Smith, 1970), and the temperature and pressure dependence of the gas properties was accounted for in the computations.

While the upper and lower extreme solutions (that is, the boundaries of the hysteresis loops)of the multiple steady state problems could be computed from the above steady state model [by providing two extreme initial guesses ($c = c_x$ and $c = 0$) which caused the single-pellet solutions to converge to one of the two extreme solutions], the use of a transient model was necessary to describe the stable, intermediate steady states of the reactor which were discovered during the course of our experimentation. The transient model ensured that only the stable solutions were found.

The transient model is a direct extension of Equation (1), with the addition of a time derivative

$$\frac{1}{r^2}\frac{\partial}{\partial r}\left\{ D(r) r^2 \frac{\partial c}{\partial r} \right\} - a(r)\tilde{R} = \epsilon_p(r) \frac{\partial c}{\partial t} \quad (20)$$

The boundary conditions are given by Equation (3) for the pellet's outer surface and by

$$\frac{dc}{dr}(0) = 0 \quad (21)$$

for the pellet's center. That is, the inert zone 1 participates in the transient process and had to be incorporated in Equation (20).

The transient response of the interpellet space was neglected, owing to its eighty times smaller time constant with respect to the intrapellet transients.

The system of partial differential equations describing

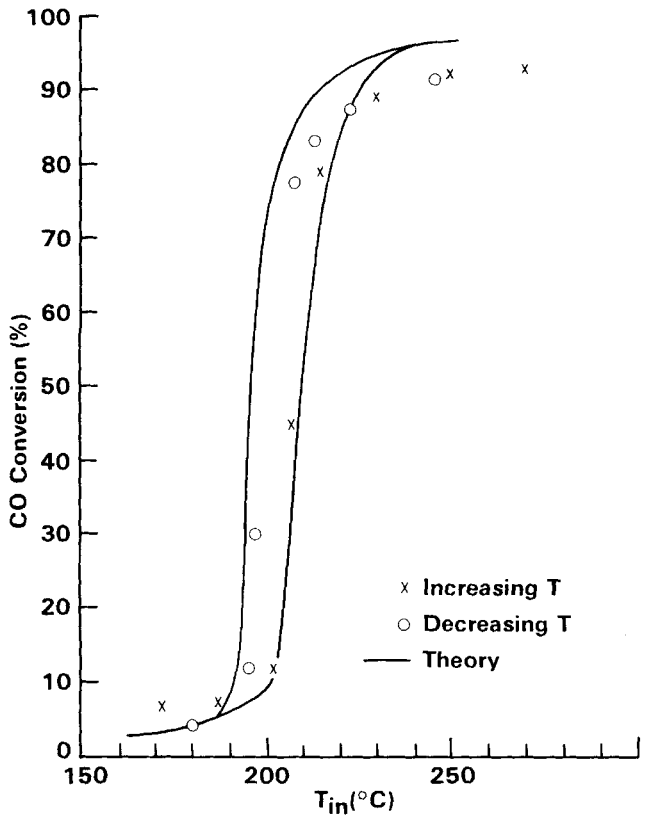

Fig. 3. Conversion-temperature behavior of a fresh catalyst (A1). Details are shown in Tables 1 and 2.

the various zones of the individual pellets was reduced to a large set of ordinary differential equations in the time domain by using the Ritz-Galerkin technique (see, for example, Hegedus and Cavendish, 1976, for the steady state problem). These were then solved by the GEARIB routine (Hindmarsh, 1976) which was designed to handle stiff problems such as this one. The numerical technique will be discussed separately.

RESULTS AND DISCUSSION

Conversion-Temperature Experiments

Figures 3 and 4 show the conversion of carbon monoxide as a function of temperature, for the fresh catalyst A1 and for its aged counterpart A2, respectively. The details of the experimental conditions and the parameters used for the computations are displayed in Tables 1 and 2. When we consider the complexity of the catalysts and the difficulty associated with quantitative catalytic experiments, a good agreement was obtained between the measured and calculated values of both catalysts. Both theory and experiment show multiple solutions for the fresh and aged catalysts alike. The temperature range in which multiple solutions can occur widens quite significantly upon catalyst aging. This widening of the range of multiple solutions is caused by modifying the diffusion-reaction process upon catalyst aging, in this case by poisoning and partially plugging an outer skin of catalyst A2.

It is of interest to discuss the reproducibility of the hysteresis curve in Figure 3 and of the curves in the subsequent figures. We found that after a given pretreatment, the curves are reasonably well reproducible. Repeated pretreatments tended to cause a small shift of the hysteresis loops (about $\pm 10°C$ on the T axis) without significantly changing their shape or area.

We also investigated a catalyst (B2, with its fresh counterpart B1) which was poisoned by a process which did not plug its pores. Such poisoning processes are more typical in automotive exhaust control applications. Figure 5 shows that the fresh catalyst has a range of multiplicities in the conversion-temperature domain which widens significantly upon poisoning (Figure 6).

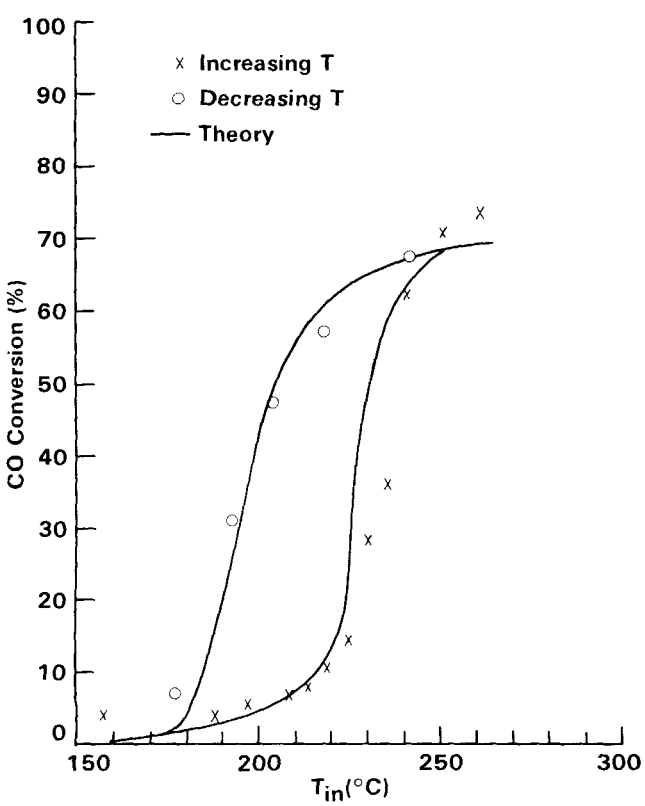

Fig. 4. Conversion-temperature behavior of an aged catalyst (A2) See Tables 1 and 2 for details.

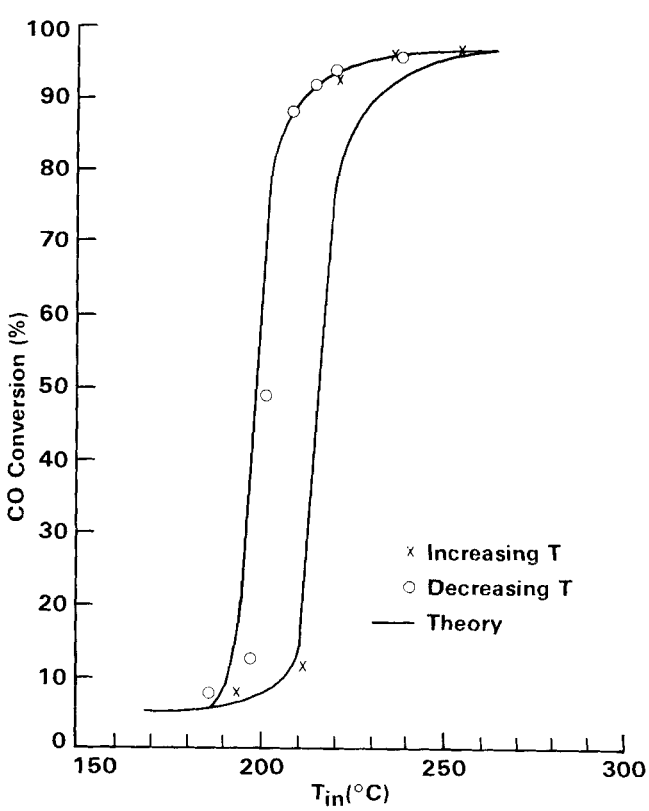

Fig. 5. Conversion-temperature behavior of the fresh catalyst (B1). See Tables 1 and 2 for details.

Independent experiments (Hegedus and Summers, 1975) showed that the phosphorus poisoned shell of platinum catalysts sometimes retains a fraction of its original activity, which becomes apparent at higher temperatures. For the conditions under which catalyst B2 was poisoned, one-twentieth of the original activity was retained, with no change in the value of the energy of activation (Schlatter, 1976). Therefore, an activity one-twentieth of the unpoisoned zone 2 was assigned to the poisoned zone 3 of catalyst B2. A comparison of this model with conversion-temperature data (Figures 5 and 6) indicates that not only severe pore plugging (as in Figure 4) but also poisoning alone can contribute to the widening of the temperature range of multiple solutions. The upward sloping, high temperature conversion limit in Figure 6 is caused by the finite activity of the poisoned layer.

Conversion-Inlet Concentration Experiments

The behavior of the integral reactor with respect to the inlet carbon monoxide concentration at a fixed temperature was also investigated. Figure 7 shows the hysteresis effect of the fresh catalyst A1 at 201°C, a temperature which falls right in the middle of the zone of multiplicity in the corresponding conversion-temperature curve (Figure 3). Tables 1 and 2 contain the parameters, and a good agreement was obtained between the data and the solution of the diffusion-reaction model.

The experiment in Figure 7 began with the data point marked by START, which is at the lowest possible steady state of the reactor at the given carbon monoxide inlet concentration. The inlet concentration of carbon monoxide was then decreased step by step, until the highest steady state was observed (owing to the negative order of the reaction, the conversion increased with decreasing carbon monoxide concentrations). Upon reversal of the direction and the increase in the carbon monoxide inlet concentration, the conversion followed a new path, along the course

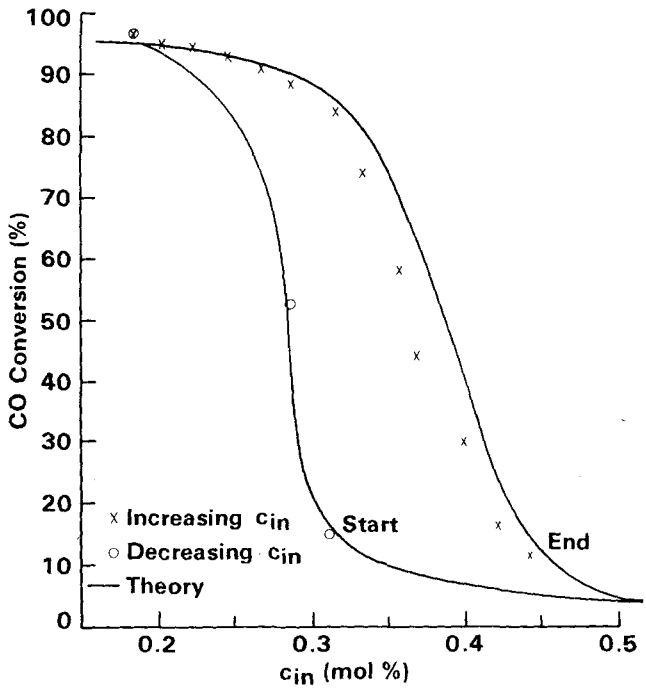

Fig. 7. Conversion-concentration hysteresis for the fresh catalyst (A1). $T = 201°C$.

of the highest steady state solution. The continuous lines in Figure 7 show the highest and lowest solutions. The theory indicates that the hysteresis loop can be closed at a high inlet carbon monoxide concentration.

Aging, as suspected from our observations to this point, will widen the range of multiplicities (Figure 8). The data are compared against calculations with two slightly different parameter sets. The high conversion (diffusion limited) calculations are especially sensitive to the value

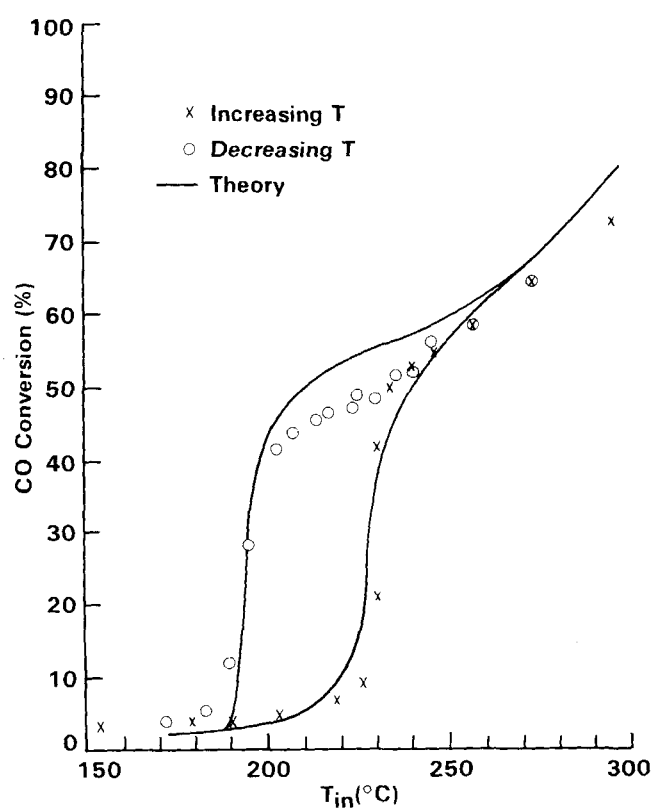

Fig. 6. Conversion-temperature behavior of an aged catalyst (B2). See Tables 1 and 2 for details.

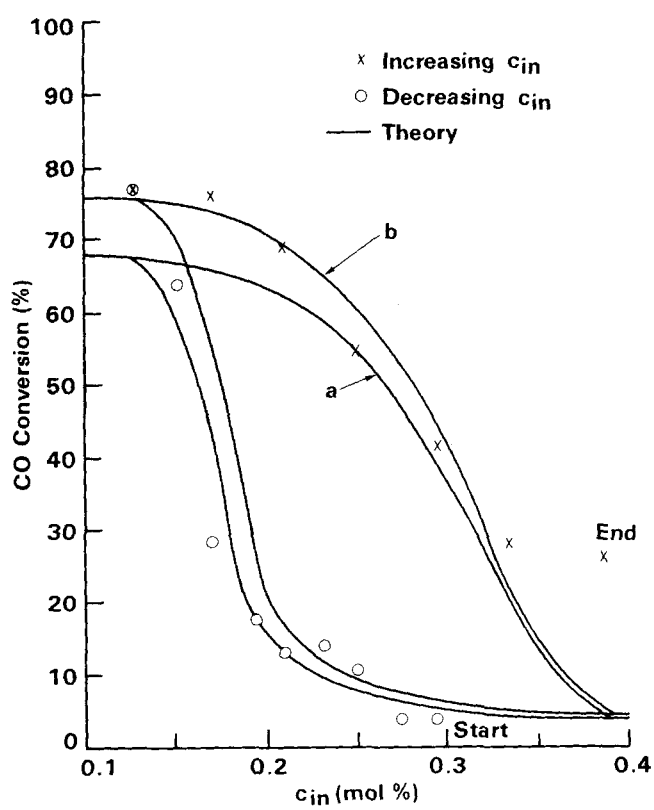

Fig. 8. Conversion-concentration hysteresis for the aged catalyst (A2). $T = 215°C$, a: $D_4 = D_2/15$, $ak_0 = 1.5 \times 10^{15}$, b: $D_4 = D_2/10$, $ak_0 = 1.8 \times 10^{15}$.

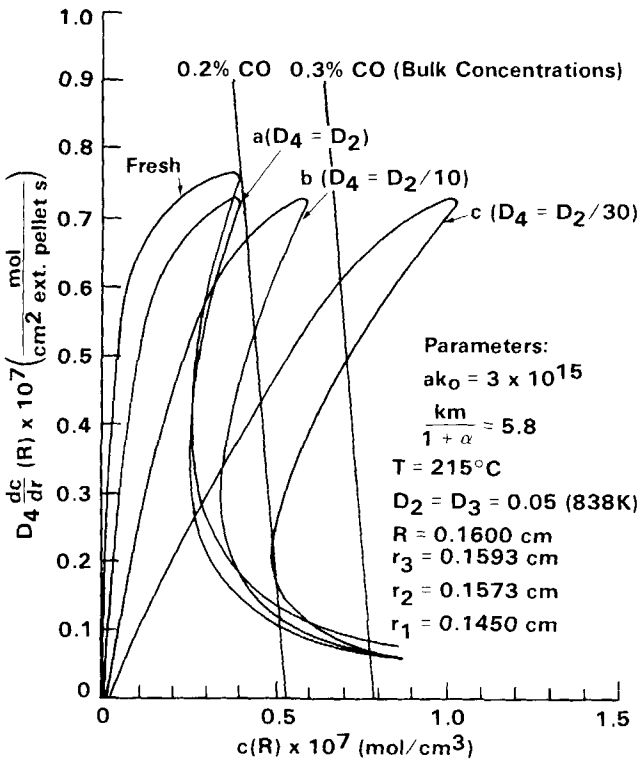

Fig. 9. Multiple solutions in a single-catalyst pellet. Note the marked effect of partial pore plugging (curves b and c). Curve a shows a partially poisoned but not plugged pellet.

of D_4, the diffusivity of the partially obstructed zone around the pellets.

It is interesting to mention that while oscillations have been often observed during carbon monoxide oxidation (for a recent review, see Sheintuch and Schmitz, 1977), we did not observe such oscillations in our integral reactor at the experimental conditions considered here. Since oscillations are primarily associated with surface phenomena, their occurrence is probably less likely in our partially diffusion limited system.

The effects of diffusion-reaction processes on the multiplicities in this system can be easily seen when the overall rate of the catalytic reaction in a single catalyst pellet (for example, as here, for a unit external pellet surface area) is plotted against the concentration of carbon monoxide at the surface of the catalyst pellet (Figure 9). In principle, this plot is similar to the qualitative diagram of Beusch et al. (1972) and Wicke (1974). It shows both the rate of the intrapellet diffusion-reaction process (curved lines) and the external mass transfer process (straight lines).

These curves can be generated without actually solving the second order boundary value problem [Equations (1) to (7)]. Instead, the solution for the first derivative can be generated by converting the boundary value problem into an initial value problem by supplying initial guesses for the concentration at the pellet's center. This approach is essentially the same as used by Weisz and Hicks (1962) to compute nonisothermal effectiveness factors in porous catalysts.

The mass transfer lines in Figure 9 are direct consequences of Equation (19). As Figure 9 shows, the external mass transfer line can cross the intrapellet diffusion-reaction line in such a way that multiple solutions occur. The maximum number of solutions is three, from which the two extreme solutions are stable and the middle one is unstable (Luss and Lee, 1971). The external mass transfer lines have been plotted at two different bulk carbon monoxide concentrations to show that even if the entrance of an isothermal reactor can only have one steady state, multiplicities still can be generated as the carbon monoxide concentration is depleted in the reactor.

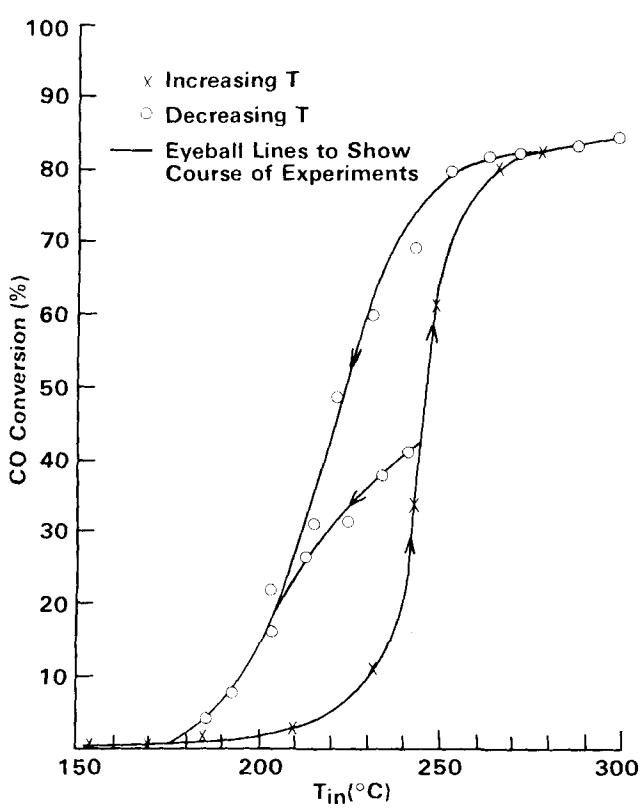

Fig. 10. Experimental demonstration of an intermediate stable steady state within the conversion-temperature envelope. See Tables 1 and 2 for experimental details (catalyst A2).

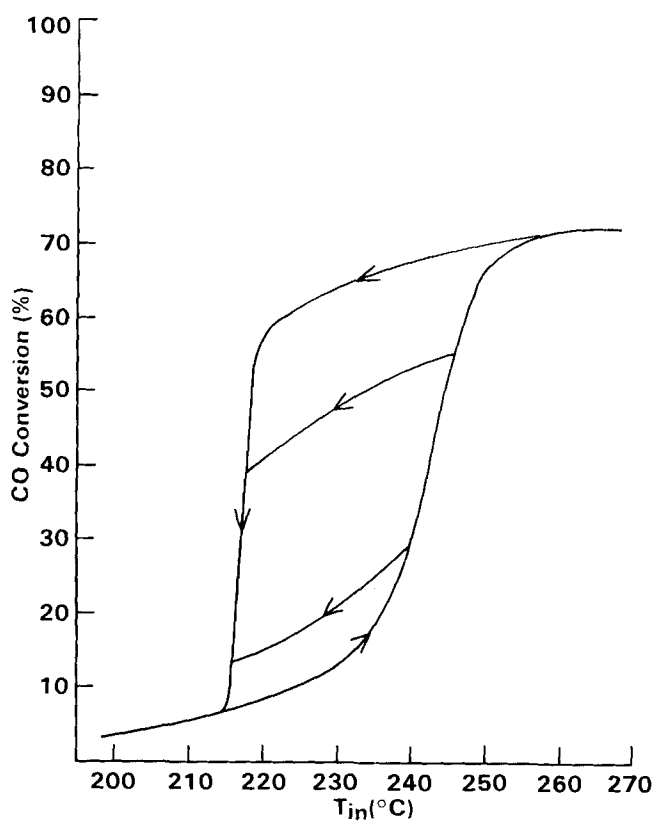

Fig. 11. Transient model simulation of intermediate stable steady states within the conversion-temperature hysteresis envelope. Tables 1 and 2 show the parameters which were employed (catalyst A2).

Figure 9 explains both the effect of poisoning and pore plugging on the multiplicities. For the fresh catalyst, the range of pellet surface concentrations in which multiplicities can occur is relatively narrow. Poisoning, and especially pore plugging, widen the region in which multiplicities can occur by appropriately modifying the diffusion-reaction process.

Are More Than Two Stable Steady States Possible?

In the experiments described up to this point, we always maintained the directionality of the forcing parameter (temperature in Figures 3 to 6, inlet concentration in Figures 7 to 8) within the region of multiple solutions. This resulted in a maximum of two stable steady states, which corresponded to the highest and lowest steady states the systems could theoretically assume (see also Eigenberger, 1972). Since adiabatic integral reactors have been predicted (Liu and Amundson, 1962) and also observed (Votruba and Hlavacek, 1974) to have more than two stable steady states, we found it interesting to investigate whether for our isothermal case, too, stable solutions inside the hysteresis loops could exist.

Figure 10 shows conversion-temperature data for the aged catalyst A2. The hysteresis envelope is the same as in Figure 4. However, one experiment was carried out in such a way that the temperature was step-by-step first increased and then reversed before the upper conversion limit was reached. As Figure 10 shows, a stable steady state curve could this way be generated inside the hysteresis envelope. The observed points appeared indeed stable: no oscillations were observed within the limits of resolution of these experiments.

The steady states within the hysteresis envelope can only be analyzed by a transient model. Step input changes were employed in the reactor temperature to retrace the course of the experiments in Figure 10. The long-time asymptotes of the transient computer solutions are plotted in Figure 11, which provides for a good qualitative comparison with the experimental data of Figure 10. (Figure 11 neglects the slight nonisothermicity of the experiments. Comparison of Figures 10 and 11 and Figures 4 and 11 demonstrates that the slight temperature gradients in the experimental reactors indeed did not change the qualitative behavior of the system as we stated in the experimental section.)

The fact that more than two stable steady states are possible in an isothermal, integral reactor with Langmuir-Hinshelwood kinetics and finite diffusion resistances can be physically interpreted by realizing that each catalyst pellet can have two stable solutions, but there are a number of pellet layers (in our case, eight) in an integral reactor and some of them may be in the lower, some of them in the higher state, similarly to adiabatic systems (see, for example, Schmitz, 1975).

It is interesting to consider the number of possible steady states within the bounds of the hysteresis envelope. For the adiabatic reactor problem with a continuum model, Liu and Amundson (1962) predicted an infinite number of stable steady states. For the same problem with a cell model, the number of stable solutions must be finite.

Stable steady states within the hysteresis envelope are also possible in the conversion-concentration domain, as Figure 12 demonstrates for the aged catalyst A2. Starting with the lowest steady state, the inlet carbon monoxide concentration was first decreased step-by-step to trace the lower envelope and then increased to move along the upper envelope.

The direction of change of the inlet carbon monoxide concentration was reversed at various points on the upper

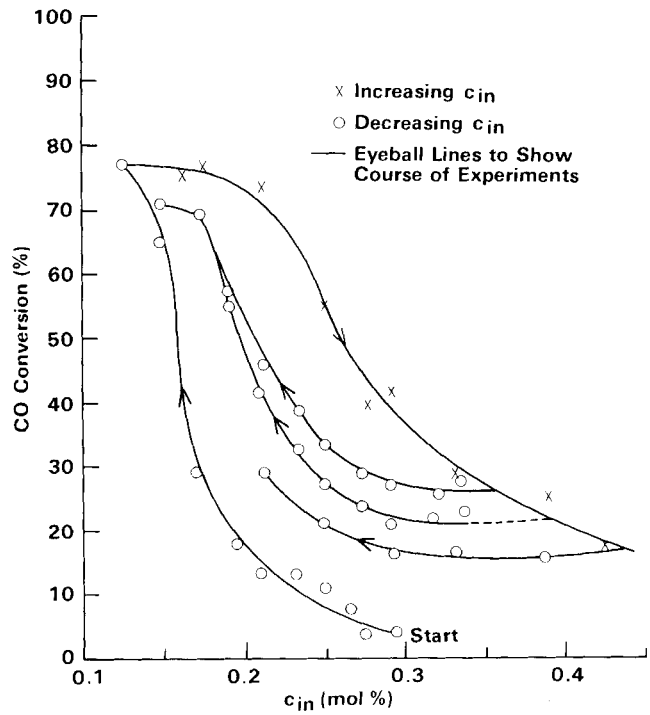

Fig. 12. Intermediate stable steady states within the conversion-inlet concentration envelope. See Tables 1 and 2 for experimental details (catalyst A2).

envelope, resulting in a family of data points inside the hysteresis loop, thus demonstrating a number of stable steady states (in this experiment, at least five) in our isothermal, integral reactor.

The existence of stable intermediate steady states within the hysteresis loop appears to be the first experimental observation of such a phenomenon for an isothermal reac-

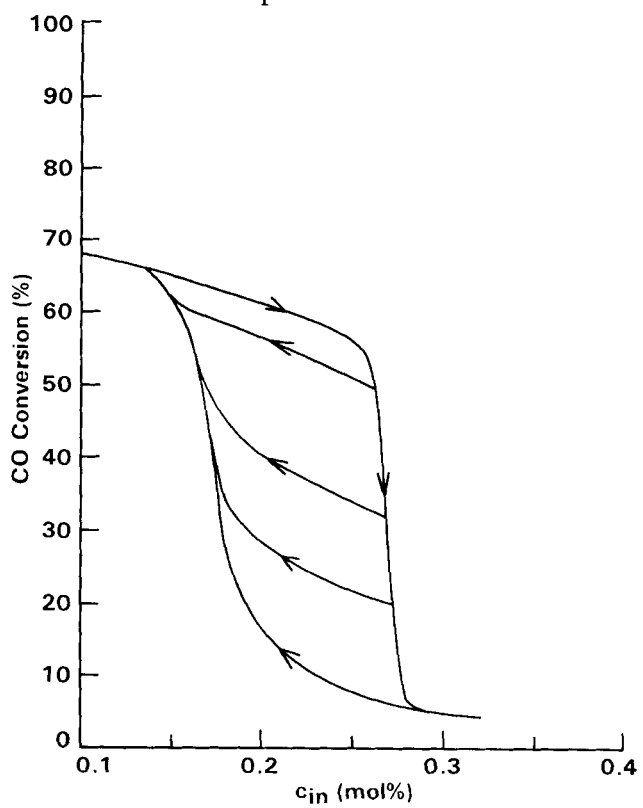

Fig. 13. Transient model simulation of intermediate stable steady states within the conversion-inlet concentration hysteresis envelope. Tables 1 and 2 show the parameters which were employed (catalyst A2).

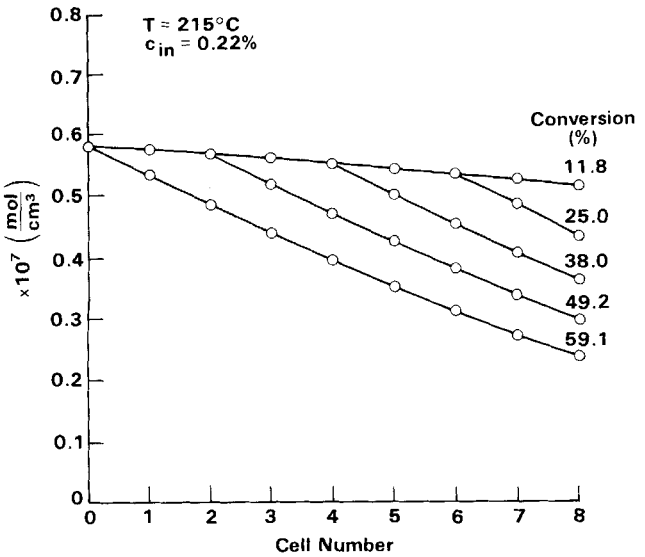

Fig. 14. Computed concentration profiles in the reactor (compare with Figure 13 at 0.22% inlet carbon monoxide concentration).

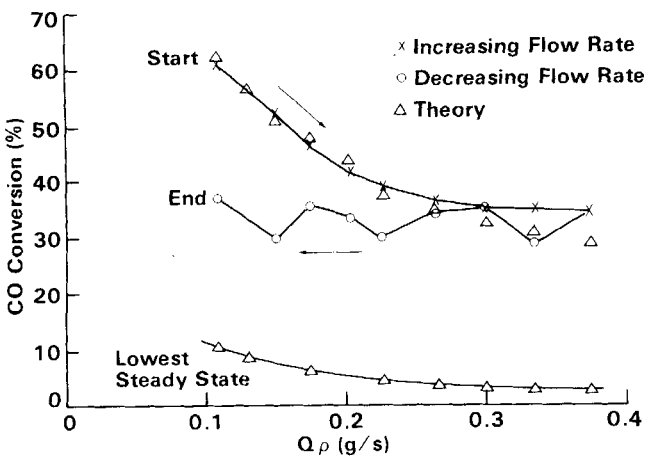

Fig. 15. Effect of feed stream mass flow rate on carbon monoxide conversion (catalyst A2), at 210°C reactor (inlet) temperature. The center curve is within the conversion-mass flow rate hysteresis envelope.

tor and was further tested by a series of experiments. In those experiments, the reactor was operated at the lowest steady state and perturbed by injecting small pulses with a reduced carbon monoxide concentration. Depending on the magnitude and duration of these pulses, the reactor assumed different stable intermediate steady states, thus verifying their existence. Details of these experiments, which include an analysis of the transient behavior of this system, will be published elsewhere.

Again, the transient model was necessary to retrace the intermediate stable steady states. The input conditions of the model followed the course of the experiments by employing a sequence of step changes in the inlet carbon monoxide concentration. The steady state limits of the numerical solutions were plotted (Figure 13, which neglects the slight nonisothermicity of the experiments).

It is worth noting that the model also predicted intermediate stable steady states when the direction of inlet concentration changes was reversed at various points on the lower branch of the conversion-inlet concentration hysteresis loop.

The experiments of Figure 12 are in qualitative agreement with the calculations (except, perhaps, the high concentration end of the data which appear to tail more than the model's predictions), again indicating that the

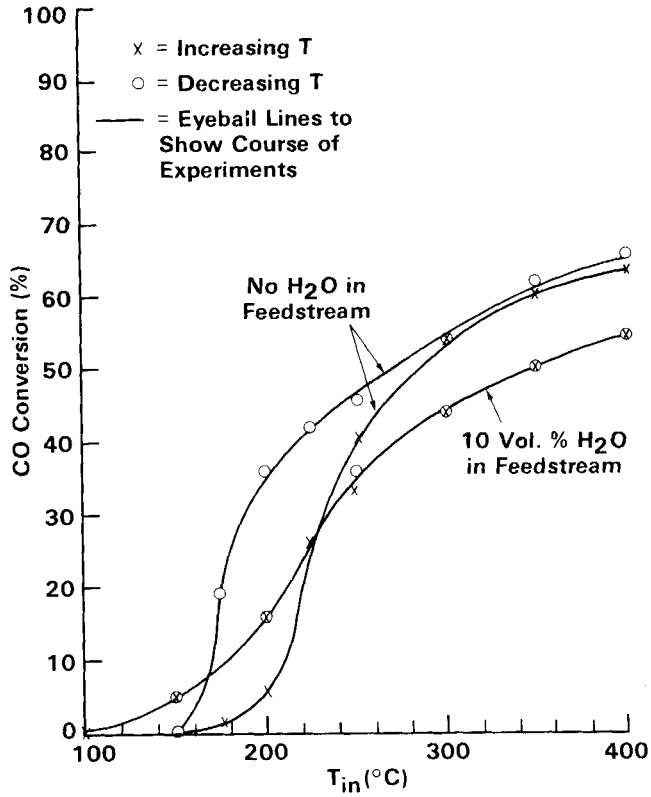

Fig. 16. Effect of water vapor in the feed stream on reactor multiplicity (catalyst A2). Parameters and experimental conditions are shown in Tables 1 and 2.

multiplicities can be well explained by isothermal reaction-diffusion theory.

It was also interesting to compute the concentration profiles in the reactor which are associated with the multiplicities. For example, Figure 14 shows the concentration profiles which were computed for the solutions shown in Figure 13 at 0.22% inlet carbon monoxide concentration. For the solutions we picked of the much larger number which are theoretically possible, the profiles show that different portions of the reactor are off and on for the different final conversions, depending on how the particular operating conditions were approached.

Experiments and calculations were also carried out to see if intermediate stable steady states can be generated by changing the mass flow rate through the reactor. Figure 15 shows the results (catalyst A2) at $T = 216°C$, well within the temperature range where multiplicities can occur (Figure 4). The reactor was set to operate at the upper steady state (compare Figures 15 and 4 at $Q\rho = 0.109$ g/s), and the mass flow rate was increased step-by-step in such a way that the inlet carbon monoxide and oxygen concentrations and the reactor temperature remained essentially constant (since they varied slightly, each point was computed separately in Figure 15 for comparison with the data). After the mass flow rate was increased to about four times its normal value, the direction of change was reversed and the mass flow rate was reduced step-by-step until its initial value was reestablished. Perhaps not surprisingly, the reverse curve does not follow the curve first established, indicating multiple solutions.

Figure 15 also shows the predicted values of lowest steady states for various mass flow rates. It should be noted that the lowest steady state conversion at $Q\rho = 0.109$ in Figure 15 is consistent with the experimental data of Figure 4. It is evident in Figure 15 that the upper set of data corresponds to the highest steady state, and

the lower set of data is in between the highest and lowest possible steady states. Thus, an intermediate stable steady state was again demonstrated by experiment, this time within the conversion-mass flow rate hysteresis envelope. The same qualitative behavior was also predicted by the transient diffusion-reaction model.

Effect of Water Vapor on Multiplicities

We mentioned earlier that the kinetic equation of Voltz et al. (1973), which was generated using water in the feed stream, did not exactly work for our experiments, and that it would predict multiplicities only at very high carbon monoxide concentrations, while our experiments with dry feed stream easily showed multiplicities at very low carbon monoxide concentrations. To test the effect of water, conversion-temperature curves were generated for the aged catalyst A2 in the absence and in the presence of 10 vol % water in the feed stream. As the results indicate (Figure 16), at 0.3 vol % inlet carbon monoxide concentration, the hysteresis completely disappears in the wet feed stream.

ACKNOWLEDGMENTS

J. C. Cavendish developed the numerical solutions employed in this paper, and the authors thank him for helpful consultations. L. L. Hegedus and S. H. Oh also thank R. Aris for stimulating discussions. The reactor experiments were carried out by E. Miller.

NOTATION

a = local platinum surface area, (cm^2 Pt/cm^3 pellet)
c = carbon monoxide concentration in the catalyst pellet, (mole/cm^3)
c_{O_2} = oxygen concentration, (mole/cm^3)
c_∞ = carbon monoxide concentration far away from catalyst pellet, (mole/cm^3)
D_i = effective diffusivity of carbon monoxide in zone i, (cm^2/s)
E = energy of activation, (cal/mole)
H = heat of carbon monoxide adsorption over platinum, (cal/mole)
k_m = mass transfer coefficient of carbon monoxide, (cm/s)
k_o = kinetic preexponential
K_o = preexponential of the carbon monoxide adsorption term
Q = gas volumetric flow rate, (cm^3/s)
$\bar{r}_{\text{macro or micro}}$ (Å) = integral averaged pore radii
r = pellet radial coordinate, (cm)
R = pellet radius, (cm)
$R - r_1$ = noble metal impregnation depth, (cm)
$R - r_2$ = poison penetration depth, (cm)
$R - r_3$ = depth of partially plugged zone, (cm)
$\tilde{R}$ = specific reaction rate, [mole/(cm^2Pt s)]
R_g = gas constant
s = BET surface area of support, (m^2/g)
T = temperature, (°K, °C)
V_{cell} = volume of a mixing cell, cm^3
$V_{\text{macro or micro}}$ = pellet pore volume, (cm^3/g)

Greek Letters

α = constant, see Equation (18)
ϵ = bed void fraction
ϵ_p = pellet void fraction
ρ = gas density, (g/cm^3)
ρ_p = pellet density, (g/cm^3 pellet)
ρ_s = pellet solid density, (g/cm^3 solid)

LITERATURE CITED

Aris, Rutherford, *The Mathematical Theory of Diffusion and Reaction in Permeable Catalysts*, Vol. I and II, Clarendon Press, Oxford, England (1975).
Beusch, H., P. Fieguth, and E. Wicke, "Thermisch und kinetisch verursachte Instabilitaten im Reaktionsverhalten einzelner Katalysatorkorner," *Chem. Ing. Tech.*, **44**, No. 7, 445 (1972).
Cardoso, M. A. A., and D. Luss, "Stability of Catalytic Wires," *Chem. Eng. Sci.*, **24**, 1699 (1969).
Dagonnier, R., and J. Nuyts, "Oscillating CO Oxidation on a Pt Surface," *J. Chem. Phys.*, **65**, No. 6, 2061 (1976).
Dauchot, J. P., and J. Van Cakenberghe, "Oscillations During Catalytic Oxidation of Carbon Monoxide on Platinum," *Nature Phys. Sci.*, **246**, 61 (1973).
Eckert, E., V. Hlavacek, M. Kubicek, and J. Sinkule, "Zur Kenntris des Zweiphasenmodells des katalytischen Reaktors," *Chem. Ing. Tech.*, **45**, No. 2, 83 (1973).
Eigenberger, G., "On the Dynamic Behavior of the Catalytic Fixed-Bed Reactor in the Region of Multiple Steady States—I. The Influence of Heat Conduction in Two-Phase Models," *Chem. Eng. Sci.*, **27**, 1909 (1972).
Fieguth, P., and E. Wicke, "Der Ubergang vom Zund/Losch-Verhalten zu stabilen Reaktionszustanden bei einem adiabatischen Rohrreaktor," *Chem. Ing. Tech.*, **43**, No. 10, 604 (1971).
Finlayson, B. A., *The Method of Weighted Residuals and Variational Principles*, Academic Press, New York (1972).
———, "Orthogonal Collocation in Chemical Reaction Engineering," *Cat. Rev. Sci. Eng.*, **10**, No. 1, 69 (1974).
Hegedus, L. L., and J. C. Cavendish, "Intrapellet Diffusivities from Integral Reactor Models and Experiments," paper presented at the 69th Annual Meeting of the AIChE, Chicago, Ill. (Dec., 1976); General Motors Research Publication GMR-2208 (July, 1976); *Ind. Eng. Chem. Fundamentals*, in press (1977).
Hegedus, L. L., and J. C. Summers, "Improving Automotive Catalysts' Tolerance to Poisoning," paper presented at the 4th North American Meeting of The Catalysis Society, Toronto, Canada (Feb., 1975); General Motors Research Publication GMR-1823 (Feb., 1975).
Hindmarsh, A. C., "GEARIB: Solution of Implicit Systems of Ordinary Differential Equations with Banded Jacobian," *Lawrence Livermore Laboratory Report UCID 30130* (Feb., 1976).
Hugo, P., "Stabilitat und Zeitverhalten von Durchfluss-Kreislauf-Reaktoren," *Ber. Bunsen-Gesellschaft fur Phys. Chem.*, **74**, 121 (1970).
———, and M. Jakubith, "Dynamisches Verhalten und Kinetik der Kohlenmonoxid-Oxidation am Platin-Katalysator," *Chem. Ing. Tech.* **44**, No. 6, 383 (1972).
Liu, S. L., and N. R. Amundson, "Stability of Adiabatic Packed Bed Reactors. An Elementary Treatment," *Ind. Eng. Chem. Fundamentals*, **1**, No. 3, 200 (1962).
Luss, D., and J. C. M. Lee, "Stability of an Isothermal Catalytic Reaction with Complex Rate Expression," *Chem. Eng. Sci.*, **26**, 1433 (1971).
McCarthy, E., J. Zahradnik, G. C. Kuczynski, and J. J. Carberry, "Some Unique Aspects of CO Oxidation on Supported Pt," *J. Catalysis*, **39**, 29 (1975).
Padberg, G., and E. Wicke, "Stabiles und instabiles Verhalten eines adiabatischen Rohrreaktors am Beispiel der katalytischen CO-Oxidation," *Chem. Eng. Sci.*, **22**, 1035 (1967).
Roberts, G. W., and C. N. Satterfield, "Effectiveness Factor for Porous Catalysts. Langmuir-Hinshelwood Kinetic Expressions for Bimolecular Surface Reactions," *Ind. Eng. Chem. Fundamentals*, **5**, 317 (1966).
Schlatter, J. C., Private communications, General Motors Research Laboratories, Warren, Mich. (1976).
Schmitz, R. A., "Multiplicity, Stability, and Sensitivity of States in Chemically Reacting Systems—A Review," *Advances in Chemistry Series*, **148**, 156 (1975).
Schneider, P., and P. Mitschka, "Effect of Internal Diffusion on Catalytic Reactions—IV. Reversible Second-Order Reaction with Langmuir-Hinshelwood Type of Rate Equation," *Coll. Czech. Chem. Commun., Engl. Edit.*, 31, 3677 (1966).
Sheintuch, M., and R. A. Schmitz, "Oscillations in Catalytic Reactions," *Cat. Rev. Sci. Eng.*, to be published (1977).

Smith, J. M., *Chemical Engineering Kinetics*, McGraw-Hill, New York (1970).
Smith, T. G., J. Zahradnik, and J. J. Carberry, "Non-Isothermal Inter-Intraphase Effectiveness Factors for Negative Order Kinetics—CO Oxidation Over Pt," *Chem. Eng. Sci.*, **30**, 763 (1975).
Voltz, S. E., C. R. Morgan, D. Liederman, and S. M. Jacob, "Kinetic Study of Carbon Monoxide and Propylene Oxidation on Platinum Catalysts," *Ind. Eng. Chem. Prod. Res. Develop.*, **12**, 294 (1973).
Votruba, J., and V. Hlavacek, "Experimental Study of Multiple States in a Tubular Adiabatic Reactor," *Inter. Chem. Eng.*, **14**, No. 3, 461 (1974).
———, and J. Sinkule, "Experimental Observation of Multiple Steady States for Diluted and Blended Catalyst Beds," *Chem. Eng. Sci.*, **31**, 971 (1976).
Wei, J., "The Catalytic Muffler," Chemical Reaction Engineering Reviews, *Advances in Chemistry Series*, **148**, 1 (1975*a*).
———, "Catalysis for Motor Vehicle Emissions," *Advances in Catalysis*, **24**, 57 (1975*b*).
———, and E. R. Becker, "The Optimum Distribution of Catalytic Material on Support Layers in Automotive Catalysis," *Advances in Chemistry Series*, **143**, 116 (1975).
Weisz, P. B., and J. S. Hicks, "The Behavior of Porous Catalyst Particles in View of Internal Mass and Heat Diffusion Effects," *Chem. Eng. Sci.*, **17**, 265 (1962).
Wicke, E., "Instabile Reaktionszustande bei der heterogenen Katalyse," *Chem. Ing. Tech.*, **46**, No. 9, 365 (1974).

Manuscript received April 8, 1977; revision received June 3, and accepted June 17, 1977.

Estimation of Flows and Temperatures in Process Networks

G. M. STANLEY
and
R. S. H. MAH
Northwestern University
Evanston, Illinois 60201

It is shown that temperatures and flows in a process network can be estimated from a quasi steady state model and a discrete Kalman filter. The data needed for such an application are readily available in many operating plants, and the computational requirements are within the capabilities of available process computers.

SCOPE

In the course of daily operation of a petroleum refinery or chemical complex, many thousands of items of information are generated, gathered, and recorded. These data are, in turn, used to plan, schedule, control, and evaluate process operations. Because of the highly integrated nature of modern processes, inaccurate data taken from one part of the process can easily lead to poor decisions which affect other parts of the processes. For instance, if inventory and production data on one product are inaccurate, the manufacturer may be forced to substitute a premium grade product to meet his delivery, thereby incurring a quality giveaway and creating an additional demand for the substitute product. Or, he may have to procure the supply from some other sources at additional costs. Or, he may accumulate unnecessarily large inventory, thereby tying up production and storage facilities needed for other products. Because of the immense scale of operations, even a small percentage change in inventory or flow may make a substantial difference in revenues or profits. The availability of accurate and consistent process data is therefore crucial to all process analyses.

Correspondence concerning this paper should be addressed to Richard S. H. Mah. G. M. Stanley is with Exxon Chemical Company, Linden, New Jersey.

In a previous paper (Mah et al., 1976), we have shown how the constraints imposed by an integrated process could be turned to advantage in enhancing the information content of the raw process data. Specifically, we showed how the overall data enhancement problem involving redundant but inconsistent data on the one hand and missing measurements on the other hand can always be resolved into two disjoint subproblems which can then be readily solved. We also showed how gross errors such as leaks and measurement biases may be detected and identified. These results were derived for flow and inventory data in a process network and based on the availability of a single set of measurements.

In this paper the treatment is extended to cover estimation of temperatures and energy flows as well as material flows in a process network. Even more importantly, the proposed estimator takes advantage of continual updates of measurements as well as the aforementioned redundancy. The estimator is designed to possess functional attributes which are judged desirable on the basis of process data collected from the atmospheric crude distillation unit of an operating refinery. The performance characteristics and computational requirements of such an estimator were investigated by simulation experiments.